Integrated V2G, G2V, and Renewable Energy Sources Coordination over a Converged Fiber-Wireless Broadband Access Network

Da Qian Xu and Géza Joós, Department of Electrical and Computer Engineering, McGill University
Martin Lévesque and Martin Maier, Optical Zeitgeist Laboratory, INRS

***Abstract*—In this paper, an integrated vehicle-to-grid, grid-to-vehicle, and renewable energy sources (IntVGR) coordination algorithm is proposed. The focus of this work is to provide a multidisciplinary study on implementing the proposed IntVGR scheme over a broadband fiber-wireless communications infrastructure by co-simulating both power and communications perspectives. For the power systems perspective, results show that the scheme is able to achieve a 21% reduction in peak demand compared to uncontrolled charging, and a better performance in flattening the overall demand profile and maintaining network constraints in comparison to a benchmark scenario. The scheme has also been demonstrated to successfully coordinate PEVs to take maximum utilization of local renewable energy. For the communications perspective, the measured upstream traffic for executing the proposed IntVGR scheme on a residential area of 342 households is found to be 1-2 Mbps with an end-to-end latency level of 1 ms. The scheme has also been validated from both perspectives in a sensitivity analysis with a higher PEV adoption rate.**

***Index Terms*—Co-simulation, demand side management, plug-in electric vehicles, smart grid communications.**

I. Introduction

THE EMERGENCE of plug-in electric vehicles (PEVs) is envisioned to become a promising alternative to conventional fuel-based automobiles. Proliferation of PEVs, however, provokes new challenges to the current electric power systems operation and planning, especially at the low-voltage (LV) distribution level from the perspective of demand side management (DSM) [1]. Charging activities of PEVs with poor regulation might impose severe stress on the distribution grid, resulting in degraded system efficiency and deterioration of power quality on a local scale [2]–[4].

In order to mitigate the aforementioned detrimental impacts due to PEV loads, some recent works have proposed various optimized and coordinated charging strategies from the viewpoint of different stakeholders, based on minimization of system-level power losses [5], [6], minimization of charging costs for PEV owners [7], and maximization of the state-of-charge (SOC) level of PEV batteries [8].

Next-generation PEVs with vehicle-to-grid (V2G) technology enabled, in addition to simply acting as a load operated in the grid-to-vehicle (G2V) charging mode, are of great potential to offer many benefits to the power grid, including peak shaving and load leveling, voltage regulation, providing frequency regulation and other ancillary services (e.g., spinning reserves), and serving as distributed storage units for backup capacity [9]. The authors in [10] propose a coordinated charging and discharging scheme based on minimization of PEV charging costs, whilst taking network constraints into account such as voltage profile patterns along the grid.

The most sustainable solution toward deployment of PEVs is to realize "Green E-mobility" by combining PEVs with renewable energy sources (RESs). PEVs are able to serve as dispersed energy storage units and help integrate RESs in the energy mix as stable base load generation capacity by performing controlled G2V/V2G operations. They can also be controlled as flexible loads to utilize local RES capacity to avoid requiring long-distance transport of electricity, reduce the risk of inducing local grid problems, and minimize the charging cost for PEV owners as well [11].

Realization of coordination of G2V, V2G, and RESs as previously discussed, relies on the creation of a bi-directional smart grid communications infrastructure capable of handling all kinds of information that needs to be exchanged among different entities [3]. As stated in IEEE P2030 released recently [12], there is a strong need to study the future power grid and its applications in a comprehensive manner that considers power systems, communications, and information technologies as a whole physical-cyber system. All the aforementioned researches, however, have focused on proposing or optimizing PEV coordination algorithms only from the perspective of power systems, while neglecting the requirement and performance of the supporting communications network. The problem states that a multidisciplinary study is required, which has also been considered one of the main challenges for future DSM [13].

In this paper, we extend our previous work [14] by proposing an integrated V2G, G2V, and RESs (IntVGR) coordination scheme, which is supported by a converged fiber-wireless (FiWi) communications infrastructure, and examining its performance from both power systems and communications perspectives in a co-simulation environment developed in our recent work [15]. The main contributions of this paper are as follows:

- The proposed IntVGR scheme aims to smoothen the overall demand profile (peak shaving and valley filling) and make maximum utilization of local RES capacity by coordinating PEVs between V2G and G2V operation

This work was supported by NSERC Strategic Project Grant No. 413427-2011, FQRNT Doctoral Research Scholarship No. 165516, and AUTO21 Network of Centers of Excellence.

Corresponding author: Da Qian Xu, McGill University, Montréal, QC, Canada H3A 0G4 (email: da.xu@mail.mcgill.ca).

modes, whilst taking into account both power grid technical constraints and PEV owners' requests and satisfaction.
- Implementation of the proposed scheme is based on exchanging notification and control packets between PEVs, households, and a central controlling system over a converged cost-effective broadband access network based on optical fiber and wireless technologies.
- In comparison to existing studies where only the power systems perspective has been considered, this is the first work that attempts to actually implement a specific PEV coordination scheme by simulating real-time information interactions in a novel co-simulation framework, and examine its performance from both power systems and communications viewpoints.

Our co-simulation results show that, from the perspective of power systems, the proposed IntVGR scheduling scheme is able to achieve a 15% improvement compared to the uncoordinated scenario in terms of flattening the overall demand profile without compromising on PEV owner's satisfaction. The scheme is also demonstrated effective in helping PEVs utilize local RES capacity to its full extent. From the viewpoint of the supporting communications infrastructure, a throughput of 1-2 Mbps is required to execute the IntVGR scheme for a distribution grid consisting of 342 households, with a fairly low end-to-end delay of 1 ms.

The remainder of this paper is organized as follows. A description of information interactions between the power systems layer and the communications network layer for implementation of the proposed IntVGR scheme is given in Section II. Section III describes the proposed IntVGR algorithm with mathematical formulations provided. Co-simulation results are shown and discussed in Section IV. Conclusions are finally drawn in Section V.

II. Power Distribution and Communications Interactions

To implement smart PEV coordination schemes in the distribution grid, a viable bi-directional communications infrastructure beyond substations is indispensable, along with advanced information and communications technologies (ICTs). We recently proposed a FiWi communications infrastructure for distribution networks based on standardized and low-cost Ethernet passive optical network (EPON), WiMAX, and wireless mesh network technologies as well as an optical metropolitan area ring network. Due to space limitations, interested readers are referred to [16] for a detailed description of our proposed FiWi infrastructure.

As this work attempts to deploy an intelligent PEV coordination scheme by exchanging real-time information packets between the superior controlling unit and PEVs, in this section we focus on explaining some main information interactions over the FiWi network, as depicted in Fig. 1, for implementing our proposed algorithm to be described in greater details in Section III.

A. Workplace/public parking garage

When a PEV arrives at the workplace, a G2V request is sent to the distribution management system (DMS) containing its identifier, status of the battery, and its desired time to be picked up. Each PEV reaches an optical network unit (ONU) by communicating in the wireless domain with a mesh portal point (MPP). The G2V request packet is then transmitted across the EPON network after a polling period and subsequently forwarded to the DMS through the optical line terminal (OLT). Upon receiving the G2V request, the DMS schedules the charging period for that PEV based on maximum utilization of generation capacity from local RES units (described in Section III). Finally, the DMS sends back a G2V response, containing the time interval when the corresponding PEV will be charged during the parking period at the public garage. After receiving the G2V response, the corresponding PEV follows the charging schedule calculated by the DMS.

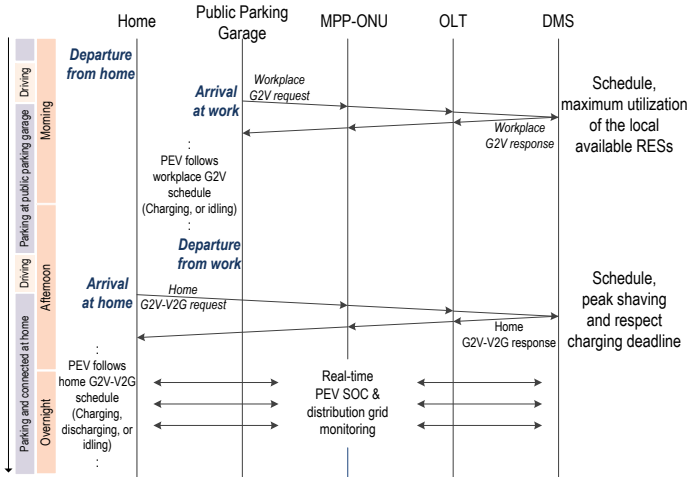

Fig. 1. Interactions between the FiWi network nodes and the DMS to implement the proposed PEV coordination algorithm.

B. Home

When a PEV arrives at home, a home G2V-V2G request message is sent to the DMS, containing its identifier, status of the battery, and deadline when the PEV is desired to be disconnected for the next trip. Upon receiving this message, the DMS performs the coordination algorithm (described in Section III) to find both the V2G and G2V slots. The central DMS then sends back the slot information to the grid-connected PEV. Finally, based on the information given in the home G2V-V2G response, a specific V2G and/or G2V schedule will be followed by the corresponding PEV to get charged, stay idle, or contribute in peak shaving together with other PEVs. Also, periodically, notification messages containing the network information such as nodal voltage magnitudes and power consumptions are sent from each household to the DMS, which might be realized by some smart metering infrastructure [15]. These messages are sent at a specific rate (denoted by λ_{notif}) depending on the required sensitivity by the utility operator.

III. Integrated V2G, G2V, and RES Scheduling Algorithm

In this section, our proposed integrated V2G, G2V, and RES (IntVGR) scheduling algorithm is described, which takes

into account not only the performance of the distribution grid but also vehicle owner's satisfaction. G2V and V2G are both considered and coordinated in such a way that better peak shaving and valley filling are realized whilst maintaining an acceptable power quality. The schematic of the proposed IntVGR algorithm with an emphasis on the part of home scheduling is illustrated in Fig. 2, which demonstrates different V2G/G2V schedules that will be assigned to a given PEV in terms of uncertainties related to its arrival time, its desirable disconnection deadline, and the amount of energy that it needs to be replenished.

To define our proposed IntVGR scheduling algorithm, we provide below the main parameters involved, objective functions, and system constraints. Note that following cost functions cannot be solved directly using an integer programming solver as multiple parameters are to be obtained by performing power flow analysis.

A. IntVGR main parameters

The main parameters of our proposed IntVGR scheduling algorithm are listed below.

- $\mathcal{H}$: Set of residential network nodes.
- $\mathcal{L}$: Set of power distribution lines.
- $t_{arr,i}$: Home arrival time of PEV i, where $i \in \mathcal{H}$.
- $t_{deadline,i}$: Deadline/disconnection time of PEV i.
- $SOC_{i,t}$: Battery SOC level of PEV i at time t.
- $P_{desired}$: Desired system-level peak demand (in kW). This is similar to the circuit level demand threshold specified in [17], which represents the network supply limit based on the existing generation capacity. $P_{desired}$ might also be a predefined level set by utility operators for other grid control purposes.
- $t_{V2G,S}$ and $t_{V2G,E}$: Start time and end time of the V2G period, which are defined as the time point when the system-level base load demand (non-PEV load consumption) becomes higher and drops lower than $P_{desired}$, respectively. $t_{V2G,S}$ and $t_{V2G,E}$ are known parameters prior to the optimization process based on historical residential base load profiles (discussed in co-simulation configurations in Section IV) and the predefined $P_{desired}$.
- T_{slot}: Interval of time slot. The time frame $\mathcal{T}$ is discretized into time slots for convenience of calculation and ease of implementation.

B. Objective function

The objectives of the proposed IntVGR algorithm are different for home scheduling and coordination at public parking garages, which will be explained and mathematically formulated in this section.

1) Home V2G scheduling: The objective for home scheduling within the V2G period is to shave the peak demand to the level of $P_{desired}$ as close as possible by aggregating feasible PEVs to feed energy back to the grid and is expressed as follows:

$$min \left(\sum_{t=t_{V2G,S}}^{t_{V2G,E}} \left(\sum_{k}^{|\mathcal{H}|} P_{k,t} - P_{desired} \right)^2 \right), \quad \forall k \in \mathcal{H}, t \in [t_{V2G,S}, t_{V2G,E}] \tag{1}$$

where $P_{k,t}$ represents the power demand at node $k \in \mathcal{H}$ at time $t \in [t_{V2G,S}, t_{V2G,E}]$. Note that $P_{k,t}$ consists of two components:

$$P_{k,t} = P_{base,k,t} + P_{PEV,k,t}, \tag{2}$$

in which $P_{base,k,t}$ denotes the base load demand at node k at time t and $P_{PEV,k,t}$ represents the PEV load and is given by:

$$P_{PEV,k,t} = \begin{cases} R_{ch} & \text{if charging at node } k \text{ at time } t \\ -R_{dis} & \text{if discharging at node } k \text{ at time } t \\ 0 & \text{otherwise} \end{cases}, \tag{3}$$

where R_{ch} and R_{dis} represent the charging and discharging power level, respectively. Note that $-R_{dis}$ indicates that the PEV is actually feeding power back to the grid as a distributed generator. It is worth noting that the aforementioned "otherwise" circumstance accounts for the situation where no PEV is assigned to node k at all or the PEV associated with node k has not yet been connected to the grid at time t, e.g., currently driving on the road. This circumstance also ensures the causality of the scheduling. For example, if PEV k arrives after $t_{V2G,S}$ (but prior to $t_{V2G,E}$), the start time of Eq. (1) for scheduling PEV k is its actual arrival time instead of $t_{V2G,S}$ because the past cannot be changed. In that case, therefore, $P_{PEV,k,t}$ equals zero for all the slots between $t_{V2G,S}$ and its arrival time, according to the "otherwise" circumstance. At any given time point t, the term $P_{PEV,k,t}$ includes all the PEVs that have already been scheduled by the DMS, and we do not consider future unscheduled PEVs in scheduling a newly arrived one.

2) Home G2V scheduling: Having determined all the discharging slots for PEV i, for G2V scheduling, the objective is to minimize the total system losses while filling the valley, which was originally proposed in [5], and can be formulated as:

$$min \left(\sum_{t}^{|\mathcal{T}-[t_{V2G,S},t_{V2G,E}]|} \left(\sum_{l}^{|\mathcal{L}|} I_{l,t}^2 \left(\sum_{k}^{|\mathcal{H}|} P_{k,t} \right) \cdot R_l \right) \right), \quad \forall k \in \mathcal{H}, t \in \mathcal{T} - [t_{V2G,S}, t_{V2G,E}] \tag{4}$$

where $I_{l,t}$ represents the current flowing along line $l \in \mathcal{L}$ at time t, and its value is obtained from load flow analysis based on the value of $P_{PEV,k,t}$ (a component of $P_{k,t}$). Note that Eq. (4) cannot be solved explicitly, but instead the optimal $P_{PEV,k,t}$ is obtained by performing iterative load flow analysis, which results in minimum system-level power losses among all the scheduling permutations.

It is worth emphasizing that the decision variable for Eqs. (1) and (4) is the slot assignment represented by $P_{PEV,k,t}$, i.e., charging, discharging, or being idle, according to Eq. (3)

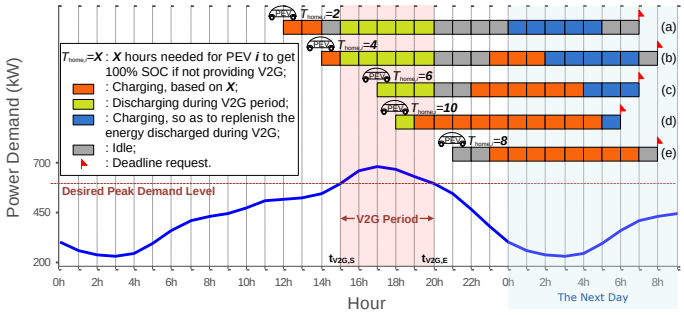

Fig. 2. Schematic of the proposed scheduling algorithm.

for all the time slots when the corresponding PEV is grid-connected. Charging and discharging power levels (R_{ch} and R_{dis}) are not decision variables, but instead they are fixed at the maximum power ratings for ease of calculation. Adjustable charging/discharging rates might be adopted, which would result in more scheduling flexibility at the expense of higher computation complexity.

3) Workplace scheduling with RES: When RES units are available at the public parking garage/workplace, the objective is to make maximum utilization of available solar power generated locally. In case that there is a shortage of RES generation, given the fact that the majority of PEVs will be parking at the garage for a long period during the day (e.g., the typical daily work duration is approximately 8 hours), some PEVs might be postponed to a later time when the generation capacity from PV panels rises (i.e., solar intensity reaches its highest level around noon time). Consequently, the overall charging profile at the parking garage will track and match the RES unit output profile by controlling the charging time of garage-connected PEVs. The objective function can be therefore formulated as:

$$min\left(\sum_{t}^{|\mathcal{T}|}\left(P_{RES,t}-P_{garage,t}\right)^2\right), \tag{5}$$

where $P_{RES,t}$ represents the power generated locally from RES units at time t, and $P_{garage,t}$ denotes the total PEV charging load at public garages at time t. Note that each PEV will be parked at the public parking garage for a specific duration of time. The algorithm attempts to postpone, if necessary, those PEVs with longer parking duration and higher SOC level, in order to ensure that all PEVs have reached a full or near-full SOC level upon being picked up by the vehicle owner and thereby to alleviate the stress on the distribution grid during peak hours.

C. Constraints

The following constraints are considered in the proposed IntVGR algorithm:

(i) To ensure an acceptable power quality at the household utilization level, the per-unit magnitude of voltage at each node must be always maintained within the acceptable range given by [18]:

$$V_{min} \leq V_{k,t} \leq V_{max}, \forall k \in \mathcal{H}, t \in \mathcal{T}, \tag{6}$$

where V_{min} and V_{max} represent the minimum and maximum limit, respectively. Note that as the distribution grid topology in this study is based on single phase, asymmetric voltage on the other phase due to PEV loads is not considered.

(ii) The total system-level power demand can not be higher than the original base load peak demand level P_{orig} at all times:

$$\sum_{k}^{|\mathcal{H}|} P_{k,t} \leq P_{orig}, \forall t \in \mathcal{T}. \tag{7}$$

(iii) To optimize the battery lifetime, the battery can never be over-charged (SOC_{max}) or over-depleted (SOC_{min}):

$$SOC_{min} \leq SOC_{i,t} \leq SOC_{max}, \forall i \in \mathcal{N}, t \in \mathcal{T}, \tag{8}$$

where $SOC_{i,t}$ denotes the battery SOC of PEV i at time t.

(iv) For each PEV i, the number of charging as usual, discharging and idle slots scheduled by the proposed algorithm, denoted by $N_{ch,i}$, $N_{dis,i}$, and $N_{idle,i}$, respectively, should satisfy the following relationship:

$$N_{ch,i} + 2 \cdot N_{dis,i} + N_{idle,i} = \left(\frac{t_{deadline,i} - t_{arr,i}}{T_{slot}}\right), \quad \forall i \in \mathcal{N}. \tag{9}$$

Note that $N_{dis,i}$ is doubled in Eq. (9) to account for the number of charging slots for the sake of replenishing the discharged energy if R_{ch} and R_{dis} are equal.

(v) Local capacity of transformers and cables, for instance, might become barriers to the adoption rate of PEVs. Our additional impact studies, which are not provided in this paper due to space limitations, have not observed any local overloading events in the scenario of random charging for the specific distribution network in this study. Therefore, local element capacity limits will not be formulated as constraints in this paper, but might be easily taken into account for other heavily loaded distribution networks.

D. Electricity market concerns

In the future PEVs may be grouped and coordinated by some aggregating agents, especially when the V2G operation mode is enabled, due to the fact that a single PEV does not have adequate capacity to exploit business opportunities in the electricity markets. The aggregating agent can be either a utility, such as the distribution system operator (DSO), or some third party for-profit entities [19]–[21]. As previously mentioned, the aggregator as the superior controlling unit in this study is served by the DMS, which is directly controlled by the DSO [3]. The DSO has the right to schedule PEVs on the basis of its own constraints: mostly peak shaving to reduce the power variation on the transmission grid and the variation in power purchases from the power producers, but also other criteria, such as reducing power losses and asset congestions in the distribution grid.

It is worth noting that the objectives of the scheduling scheme currently proposed in this work is from the technical point of view, while electricity markets and market-based financial benefits to PEV owners or the

aggregation unit are not taken into account. Therefore, our current approach is valid in jurisdictions where no electricity markets are involved. In addition, as stated in [3] where a hierarchical technical and market management structure was proposed, our approach is also valid when the power grid is approaching its technical restrictions or the grid is operated in abnormal or emergency conditions (e.g., contingencies and islanded operation), in which case the DMS headed by the DSO will act over, and if necessary, override V2G/G2V decisions from market-oriented aggregators with pure economic interests, if there are any.

In spite of this, the authors acknowledge that it is still important for our future work to integrate electricity market features in the scheduling scheme facilitated by the aggregation unit. Some recent works have already studied the market model of the aggregator, for example, based on maximization of financial profits from providing ancillary services (frequency regulation and spinning reserves) [22] or energy trading-related profits [19]. However, these analyses were performed at the bulk power level and ignored technical constraints at the distribution level. The authors in [19] concluded that current market policies and mechanisms with regard to PEV deployment need to be revised so as to provide sufficient incentives, especially for those third-party aggregating business, to take into account the technical perspective of the power grid in order to prevent imposing detrimental impacts on grid operations due to their for-profit V2G/G2V decisions.

Under current policies, the DSO is not allowed to be able to compete with other players in the market due to its advantage of having access to the network details. Instead, as previously mentioned and discussed in [3], the DSO sees the third party aggregator as an important actor in the distribution grid operation. Prior to approving the for-profit aggregator to proceed to any market negotiation, the DSO will perform an ex ante validation of V2G/G2V decisions (sell/buy bids) proposed by the aggregation unit, and if necessary, the DSO will ask the aggregator to make proper changes on the proposal until a safe technical feasibility is guaranteed (e.g., branch congestions, voltage profiles, etc.) [20], [21]. The DSO might mandate the aggregator to make further changes on its plan according to some other grid control purposes. This is how the technical and the market perspectives are integrated.

Therefore, to integrate the electricity market perspective into our current scheduling scheme, the aforementioned technical and market management structure could be modeled. The objectives will differ from those proposed in this work, and instead the scheduling might be based on maximization of the financial profits for the aggregator by optimizing energy and ancillary service scheduling, or minimization of the charging costs for the PEV owner [21]. The technical aspects, i.e., network constraints and some specific targets imposed by the DSO for a given feeder, such as peak shaving and minimized power losses as formulated in Eqs. (1) and (4), can be easily integrated into the optimization formulation by adapting the objective functions to additional constraints. These technical constraints, however, do not imply that the aggregator will have access to the network details as the DSO does, but rather represent the aforementioned ex ante validation procedure by the DSO, which ensures a safe grid operation. Another option to deal with the technical perspective might be based on transforming the technical constraints into equivalent monetary costs and keep them also in the objective function, similar to the work in [23].

It is worth emphasizing that the main focus of this work is on co-simulating the information interactions required to facilitate a specific PEV scheduling scheme and examining its performance from both power systems and communications viewpoints. In our future work, hence, instead of combining the technical and the market perspectives together in the scheduling formulation as previously explained, it is also possible to co-simulate the interactions among all the involved entities within the technical and market management framework, where the ex ante proposal/validation process between the DSO and the for-profit aggregator will also be modeled by simulating the information exchange between them, and to investigate the impacts of the scheduling decisions from the for-profit aggregator on the distribution grid operations and constraints.

IV. Co-simulation Results

This section provides co-simulation results for our proposed IntVGR scheduling algorithm. We also consider a well-performing smart charging scheme recently proposed in [5] for benchmark comparison.

A. Co-simulation configurations

The proposed IntVGR scheduling algorithm is tested in our recently developed co-simulation environment, which is built using OMNeT++, while the power systems layer is modeled and load flow analysis is performed in OpenDSS. The architecture of the co-simulation platform is explained in details in our previous work [15]. We provide below a brief summary on the specific configurations used in this paper regarding the distribution network, the FiWi communications infrastructure, and the investigated scenarios.

1) Distribution grid configurations: Our co-simulation model is configured according to the following settings for the power distribution network:

- *Distribution network topology*: The distribution network is a modified IEEE 13-node radial distribution feeder [24], as depicted in Fig. 3. It has 18 LV residential networks, each of which consists of 19 customer households, representing 342 households in total.
- *PEVs*: PEVs are modeled based on the specification of a commercial PEV model, Nissan LEAF[1] (Table I). Each PEV is associated with a specific home arrival time, home departure time, and daily driving distance based on realistic data extracted from the National Household Travel Survey (NHTS) 2001 [2].

[1]LEAF's manual is available at http://www.nissanusa.com/leaf-electric-car.
[2]The NHTS dataset is available at http://nhts.ornl.gov.

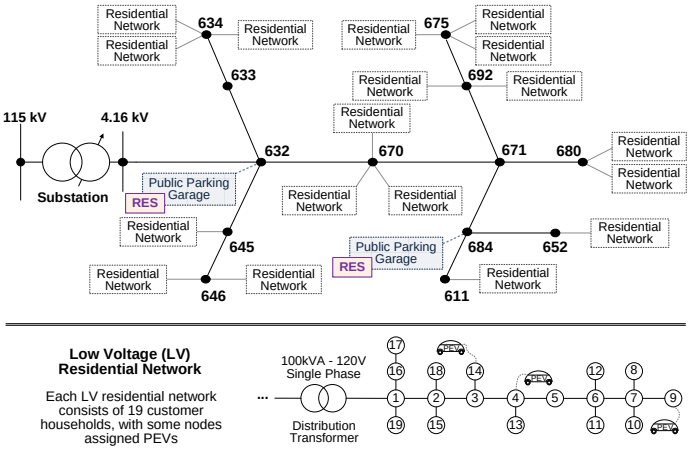

Fig. 3. Single line diagram of the 342-node distribution network topology.

- *Public parking garages*: Two public parking garages are available at node 632 and 684, respectively, where vehicle owners can park and charge their PEVs during work time.
- *RES*: PV panels are assumed available at parking garages. Each PV panel is configured to have an area of 500 m^2, with a conversion efficiency of 12% and an inverter efficiency of 95% [3]. Based on the sun irradiance level in Montréal [4], the hourly distribution of the generation capacity from PV panels can be determined, as shown in Fig. 4.
- *Residential base load*: A base load profile is applied at each household to model its daily base load consumption. The load shape is obtained from the RELOAD[5] database for both summer and winter. For each season, two additional load curves are generated by time shifting the original load shape by +/- 1 hour to account for discrepancies in residential daily routines. At each household and hour, the load randomly varies among the three aforementioned load profiles based on a uniform distribution. The maximum power demand and power factor are set to 2 kW and 0.95 [5], respectively, at each household.

TABLE I
PEV MODEL CONFIGURATION

Model	Nissan LEAF
Battery capacity	24 kWh
Maximum depletable capacity	80%
Electric drive efficiency	0.26 kWh/mile [25]
Charge/Discharge efficiency	90% [26]
Charging infrastructure	Level 1 [27]
Power rating	1.44 kW (120VAC/12A)

2) FiWi-based communications infrastructure configurations: An EPON of 32 ONUs with a line rate of 1 Gbps is used for the fiber backhaul. The ONU nodes are distributed uniformly to cover the entire distribution grid of 342 customer households. A wireless mesh network based on IEEE 802.11g with a line rate of 54 Mbps is used to aggregate sensor data for those customer households without a direct connection to an ONU. The wireless mesh network forwards their packets through the closest ONU collocated with an MPP. The notification message rate, λ_{notif}, is set to 1 message per second. Due to space limitations, we do not evaluate the impact of λ_{notif} on our proposed IntVGR scheme. Nodal voltage and power consumption measurements are assumed to be available directly without any sensing delay or error.

[3]Efficiencies are given at http://www.solarbuzz.com/.

[4]Sun irradiance level data is available at http://www.climate.weatheroffice.qc.ca/.

[5]RELOAD Database Documentation and Evaluation and Use in NEMS is available at http://www.onlocationinc.com/LoadShapesReload2001.pdf.

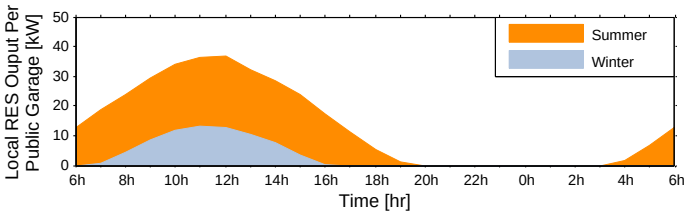

Fig. 4. Hourly distribution of the generation capacity from the local RES unit at the public parking garage (workplace).

3) Definition of investigated scenarios: Two penetration levels (PLs), i.e., 42% and 84%, are tested in the simulation. We introduce a coefficient η, which specifies the ratio of $P_{desired}$ to P_{orig}. The smaller the value of η is, the lower the peak demand level is desired and the longer the V2G period is extended. To be more specific, $P_{desired} = (342 \times 2) \cdot \eta$ in kW, where 342×2 corresponds to the system-level peak demand for non-PEV loads. η is varied from 0.80 to 0.95.

The following simulation scenarios are considered:

- *H-R:* This scenario serves as the business-as-usual (BAU) scenario, in which case PEVs are charged in a random and uncoordinated manner immediately upon arrival at home until being fully replenished, and therefore, no ICTs are involved.
- *H-S:* A smart charging scheme recently proposed in [5] is applied to home scheduling, which attempts to maintain the original base load peak demand level while minimizing the total power losses. This scenario serves as a benchmark test case for efficacy validation of the proposed IntVGR scheduling algorithm. The reason for taking this scheme as benchmark is that its objective is also from the technical viewpoint of power system (network constraints) instead of cost-benefit analysis as proposed in some other studies, and it has been demonstrated to successfully control the system peak demand level and regulate voltage deviations.
- *W-R/H-S:* Added to the aforementioned *H-S* scenario, public parking garages become available and thus enable parked PEVs to get charged in an uncoordinated manner during work hours.
- *IntVGR(η, w/o RES):* The proposed IntVGR algorithm is applied but no local RES generation unit is available.
- *IntVGR(η, w/ RES):* The proposed IntVGR is implemented with its full functionality.

4) Computation complexity: The proposed IntVGR algorithm may require a significant amount of calculations to find optimal solutions, depending on the value of parameters involved in scheduling. To decrease the computation complexity, first of all, the considered time frame, $\mathcal{T}$, must be finite, and intuitively, $\mathcal{T}$ could be set to 24 hours in order to schedule PEVs on a daily basis. Meanwhile, discretization of $\mathcal{T}$ into time slots (T_{slot}) significantly reduces the number of required power flow analyses. Furthermore, in order to cut down even more the number of calculations, we created a caching system in our co-simulator, exposed in our previous work [15], which avoids rerunning the same power flow analysis two times. In our numerical simulations, a T_{slot} of 15 minutes, which has also been suggested as a likely interval for PEV scheduling in [3], and a $\mathcal{T}$ set to 24 hours along with the aforementioned caching system have not led to a large computation time.

B. Results for the performance of distribution grid

The following performance metrics are measured and examined: (i) D_{peak} denotes the peak power demand in kW needed from the main source, (ii) L_{max} denotes the maximum system losses in kW, including both line losses and transformer losses, (iii) V_{min} represents the minimum per unit (p.u.) value of voltage at the node with the worst daily voltage profile, (iv) $V2G_{max}$ denotes the maximum power in kW fed back to the grid by aggregated PEVs, and (v) SOC_{final} indicates the average SOC in percentage upon PEV's deadline.

Table II shows the results for the aforementioned scenarios based on a PL of 42% and a summer base load profile. One of the main objectives of the proposed IntVGR algorithm is to smoothen the overall demand profile by shaving the peak. Despite that the benchmark *H-S* scenario successfully maintains the same peak level as P_{orig} (681.49 kW), our proposed IntVGR algorithm is able to achieve much more. The performance in terms of peak shaving and valley filling for different charging strategies is shown in Fig. 5. It can be observed that the *H-R* scenario increases D_{peak} significantly and the *W-R/H-R* scenario enables public parking garages to share some of the charging burden during periods of already high demand. The *H-S* scenario successfully avoids the situation where PEV charging activities coincide with household peaks. In comparison, the *IntVGR(0.90, w/o RES)* scenario achieves a peak demand even lower than P_{orig} by coordinating feasible PEVs to provide V2G services during peak hours. Fig. 6 provides a closer look at the IntVGR algorithm between G2V and V2G modes. D_{peak} is further shaved as η decreases. With η equal to 0.80, D_{peak} is brought down to 605.79 kW, decreased by 21% compared to that in the BAU scenario.

The second metric in Table II, L_{max}, is reduced by 30% from 22.65 kW in the *IntVGR(0.80, w/o RES*) scenario compared to that in the BAU scenario. The distribution system operator is concerned about power losses, which could be potentially compensated by increasing the electricity tariffs at customer premises. Based on the deployment of ICTs, intolerable voltage deviations are avoided and V_{min} at all nodes is always maintained within the acceptable limit ([0.95, 1.05] p.u under normal conditions), as shown in Fig. 7. Compared to the benchmark *H-S* scenario, the proposed IntVGR algorithm achieves a better performance in voltage regulation.

It is worth noting that for some η, $P_{desired}$ cannot be always reached. For example, with η equal to 0.80, D_{peak} is only shaved to 605.79 kW, or equivalently 85% of D_{orig}, and $V2G_{max}$ increases by only 4.32 kW, corresponding to three more PEVs, as η decreases from 0.85 to 0.80. This can be explained by the fact that our proposed IntVGR algorithm also takes PEV owner's need into account, which is illustrated in Fig. 8. It can also be observed from Table II that SOC_{final} is not sacrificed but maintained at a fairly satisfying level (above 99.88%).

Another objective of the proposed IntVGR algorithm is to take maximum utilization of low-cost energy generated locally from RES units, considering the fact that most PEVs are parked for quite a long period during the day and as such give sufficient flexibility of their charging time. As shown in Fig. 9, in an uncoordinated and random manner, there is a garage charging peak at 9 a.m. due to most PEVs arriving at work around that time, and thereby, some PEVs need to take power from the grid as a result of not sufficient capacity from local RES units. The *IntVGR(0.90, w/ RES)* scenario, in contrast, is able to track the RES output profile by putting off those PEVs with relatively longer parking duration to a later time when the RES output increases. For example at 9 a.m., only 38 out of 80 PEVs are enabled by the IntVGR algorithm to charge while the remaining 42 ones are delayed. Note that with the same η, *IntVGR(η, w/ RES)* scenarios result in lower D_{peak} and $V2G_{max}$ than *IntVGR(η, w/o RES)* scenarios do, as can be observed in Table II, which can be explained by the fact that a surplus of RES output, if applicable, is fed back to the grid and to some extent contributes in peak shaving.

The sensitivity to the PEV adoption rate of our proposed IntVGR algorithm is then tested with a higher PL of 84%, the results of which are given in Table III. Besides similar results to those previously mentioned, we make some new observations. As the PL is high, a higher morning peak exists as a result of PEVs charging at public parking garages (e.g., D_{peak} is 651.40 kW in *IntVGR(η, w/o RES)* scenarios with η equal to 0.90, 0.85, and 0.80). Although the garage charging demand is more than the amount that local RES units can provide, the IntVGR algorithm makes its best effort in coordinating PEVs for utilization of local renewables and preventing the occurrence of the aforementioned peak during morning hours, as depicted in Fig. 10.

As the PL rises, more efforts are required to aggregate PEVs to provide V2G services. We note that as the PL is doubled from 42% to 84%, $V2G_{max}$, however, is not doubled, which can be explained by the fact that a higher PL results in a higher probability that PEVs have to be interrupted from V2G mode and switched back to G2V mode within the V2G period for the sake of reaching a satisfying SOC level by the desired deadline. As observed in Table III, SOC_{final} is slightly worsened by only 1%.

We also validate the efficacy of our proposed algorithm with a winter base load profile. Similar findings to Table II and III were obtained, but results are not given in this paper due to

TABLE II
CO-SIMULATION RESULTS FOR A PL OF 42% AND A SUMMER BASE LOAD PROFILE.

	w/o ICTs	w/ ICTs									
	H-R	*H-S*		*IntVGR(η, w/o RES)*				*IntVGR(η, w/ RES)*			
		w/o *W-R*	w/ *W-R*	η=0.95	η=0.90	η=0.85	η=0.80	η=0.95	η=0.90	η=0.85	η=0.80
D_{peak} [kw]	759.87	681.49	678.16	666.54	635.20	633.84	605.79	653.27	630.55	609.09	584.09
L_{max} [kw]	32.34	27.22	26.90	26.12	24.05	24.00	22.65	26.29	24.59	23.92	22.49
V_{min} [pu]	0.9443	0.9507	0.9531	0.9522	0.9548	0.9553	0.9558	0.9521	0.9528	0.9528	0.9552
$V2G_{max}$ [kw]	0	0	0	38.88	69.12	87.84	92.16	21.60	50.40	73.44	87.84
SOC_{final} [%]	100.00	99.63	100.00	100.00	99.95	99.88	99.90	100.00	100.00	99.94	100.00

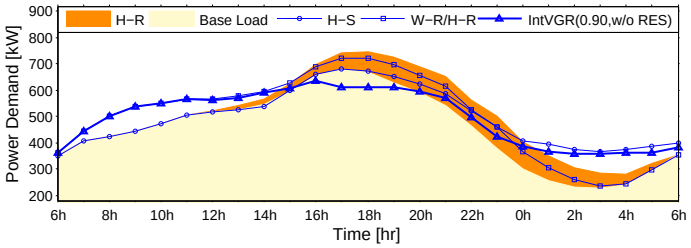

Fig. 5. The overall demand profile in different simulation scenarios based on a PEV penetration level of 42% and a summer base load profile.

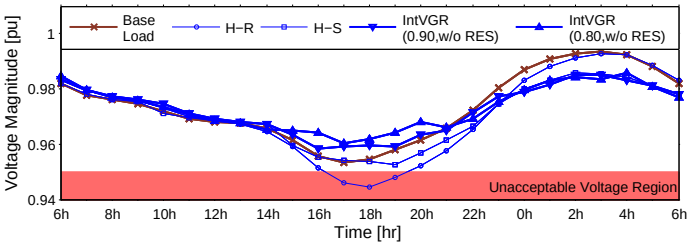

Fig. 7. Worst nodal voltage profile based on a PEV penetration level of 42% and a summer base load profile.

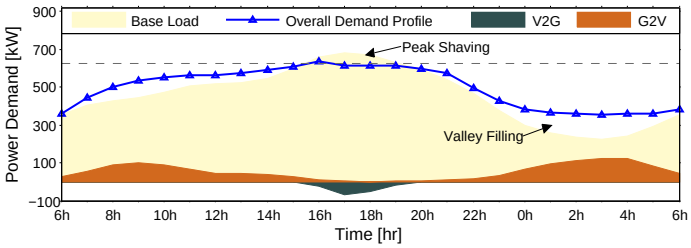

Fig. 6. Operation of G2V and V2G modes in the *IntVGR(0.90, w/o RES)* scenario based on a PEV penetration level of 42% and a summer base load profile.

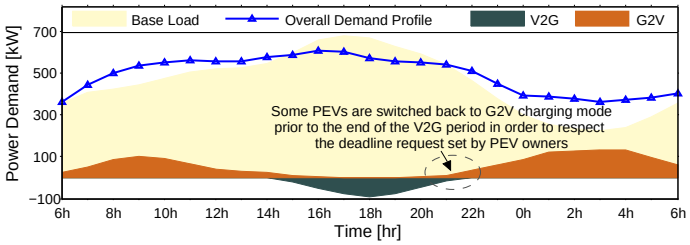

Fig. 8. Operation of G2V and V2G modes in the *IntVGR(0.80, w/o RES)* scenario based on a PEV penetration level of 42% and a summer base load profile.

space limitations.

To sum up, our proposed IntVGR algorithm has been demonstrated to successfully smoothen the overall demand profile by peak shaving and valley filling, the peak-to-average ratio (PAR) of which can be brought down to 1.28 with η equal to 0.90 and even lower as η further decreases. This is much improved compared to a PAR of 1.50 for the BAU scenario and 1.38 for the benchmark scenario, allowing the utility to run the power grid at decreased peak provisioning with higher system efficiency, lower costs, and also reduced carbon emissions. It has also been proved effective in coordinating PEV charging loads based on tracking the generation profile of local RES units. Note that in simulations, we use a forecast output profile known in advance for local RES units. To deal with unpredictable uncertainties/deviations involved in generation/load profiles, we have proposed and examined in our previous work [14] a reactive coordination scheme, which is able to adjust the scheduling results with respect to unknown variations, but this is not the main focus of this paper.

C. Interoperability with the supporting communications infrastructure

The performance of the communications infrastructure also plays a critical role for deployment of the proposed scheduling algorithm. Two main performance metrics are examined, namely, channel throughput and delay. Due to space limitations, we show selected results for the aforementioned scenarios from a communications perspective.

For all the simulation scenarios, the bandwidth utilization is observed to vary significantly with the PL and whether garage scheduling with RESs is deployed, as depicted in Fig. 11. During the simulation interval from 26 to 42 seconds, corresponding to 6 to 10 a.m. on the virtual distribution system layer (VDSL), bandwidth utilization is higher for scenarios with RESs scheduling enabled and remains unchanged if PEVs are charged in an uncoordinated manner at public garages. Note that 1 simulation second corresponds to 15 minutes on the VDSL and the interval up to 26 seconds is basically used for simulation initialization and thus not shown in the figure. During peak hours, starting from 70 seconds, the throughput significantly increases for both PLs as a large volume of home G2V-V2G requests/responses as well as other messages such as SOC information packets are exchanged between PEVs and the DMS. The channel throughput reaches the peak at around 114 seconds (4 a.m. on the VDSL). This is caused by the fact that the number of PEVs that are in charging (G2V) mode reaches the maximum at 4 a.m. and thereby the number of SOC messages exchanged between

TABLE III
CO-SIMULATION RESULTS FOR A PL OF 84% AND A SUMMER BASE LOAD PROFILE.

	w/o ICTs	w/ ICTs									
	H-R	*H-S*		*IntVGR(η, w/o RES)*				*IntVGR(η, w/ RES)*			
		w/o *W-R*	w/ *W-R*	η=0.95	η=0.90	η=0.85	η=0.80	η=0.95	η=0.90	η=0.85	η=0.80
D_{peak} [kw]	850.08	683.29	679.13	667.46	651.40	651.40	651.40	668.71	641.59	624.28	595.51
L_{max} [kw]	38.89	27.21	26.88	26.17	24.26	23.40	20.48	25.86	24.24	23.19	20.53
V_{min} [pu]	0.9397	0.9503	0.9531	0.9527	0.9536	0.9542	0.9533	0.9484	0.9518	0.9537	0.9544
$V2G_{max}$ [kw]	0	0	0	40.32	83.53	119.52	138.24	48.96	90.72	122.40	151.20
SOC_{final} [%]	99.87	98.82	99.93	99.92	99.87	99.66	99.24	99.72	99.57	99.30	98.88

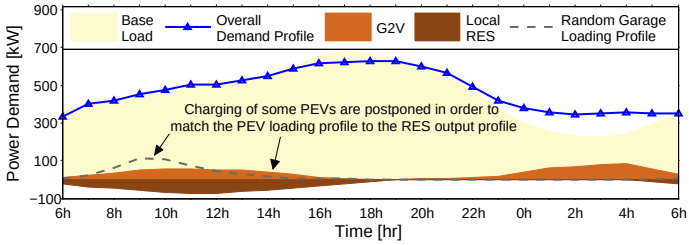

Fig. 9. Workplace scheduling with RESs in the *IntVGR(0.90, w/o RES)* scenario based on a PEV penetration level of 42% and a summer base load profile.

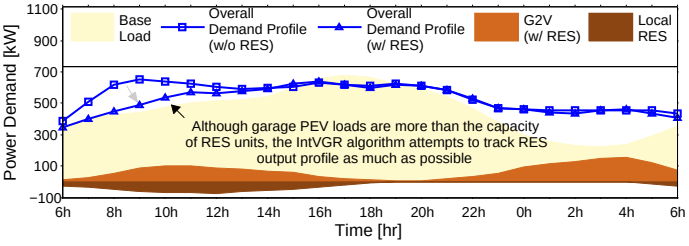

Fig. 10. Workplace scheduling with RESs based on a PEV penetration level of 84% and a summer base load profile, $\eta = 0.90$.

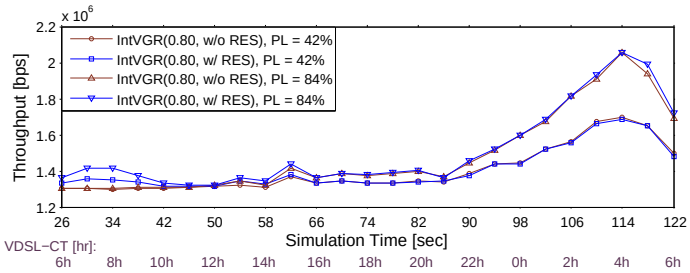

Fig. 11. Upstream throughput measured at the DMS for different PLs.

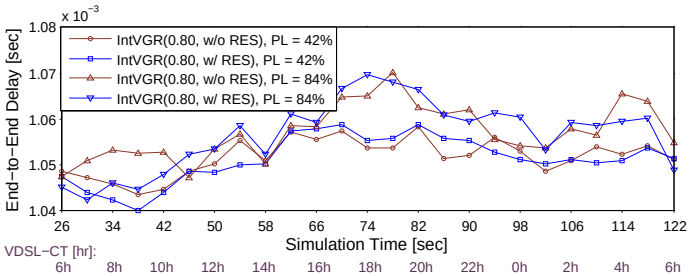

Fig. 12. Upstream end-to-end delay measured at the DMS for different PLs.

PEVs and the DMS also reaches the maximum amount, which is consistent with the findings in Fig. 8 where G2V charging load reaches the maximum at 4 a.m.. When the PL is doubled from 42% to 84%, the number of PEVs is doubled, which might explain the observation that the channel throughput due to exchanging PEV-related messages is also roughly doubled at critical time points. Note that the bandwidth taken up by information interactions other than PEV-related messages, such as notification messages containg the sensor data for grid monitoring (loads, nodal voltages, etc.), is approximately 1.3 Mbps, and it remains unchanged over time for both two PLs as the number of household is fixed.

With regard to the second metric, as shown in Fig. 12, the upstream end-to-end delay measured at the DMS is approximately 1 ms and, as expected, is slightly higher on average for a higher PL, which is consistent with observations for the channel throughput. Note that the end-to-end delay takes into account the transmission, propagation, and queuing delays. We do not evaluate computation times. The delay reaches its highest level during 66 to 90 simulation seconds (4 p.m. to 22 p.m. on the VDSL). This can be explained by the fact that most PEVs arrive at home during this period and contend for the wireless network channel bandwidth to exchange their messages to the DMS through an ONU, and therefore packet collision is more likely to occur as multiple PEVs attempt to transmit their messages to an ONU simultaneously.

Note that 1-2 Mbps were required by the proposed algorithm with the aforementioned configurations. Depending on the sensitivity required by the utility, λ_{notif} can be changed. As our proposed communications infrastructure has the potential of sharing its bandwidth with other applications, such as voice and video, quality-of-service issues could be noted. We addressed this problem in our previous work [28], to which interested readers are referred for further details.

V. CONCLUSIONS

In this paper, our proposed IntVGR algorithm has been implemented in a co-simulation environment by exchanging real-time message and data between the DMS and PEVs over a converged FiWi broadband access network. Its performance from both power systems and communications perspectives has been examined. Results demonstrate its effectiveness in smoothening the overall demand profile and controlling PEVs to make maximum utilization of local RES capacity. Grid constraints as well as vehicle owners's satisfaction are both taken into account. To deploy the proposed scheme over a distribution grid consisting of 342 customer households, the utilized upstream bandwidth is found to be 1-2 Mbps,

which occupies a fairly low level of the EPON channel resources and a low end-to-end delay of 1 ms is obtained. The multidisciplinary study performed in this paper can be further extended to accommodate various smart grid applications and services in more complex physical-cyber systems.

REFERENCES

[1] A. G. Boulanger, A. C. Chu, S. Maxx, and D. L. Waltz, "Vehicle Electrification: Status and Issues," *Proc. IEEE*, vol. 99, no. 6, pp. 1116–1138, Jun. 2011.

[2] L. Pieltain Fernández *et al.*, "Assessment of the Impact of Plug-in Electric Vehicles on Distribution Networks," *IEEE Trans. Smart Grid*, vol. 26, no. 1, pp. 206–213, Feb. 2011.

[3] J. A. P. Lopes, F. J. Soares, and P. M. R. Almeida, "Integration of Electric Vehicles in the Electric Power System," *Proc. IEEE*, vol. 99, no. 1, pp. 168–183, Jan. 2011.

[4] K. Clement-Nyns, E. Haesen, and J. Driesen, "The Impact of Charging Plug-In Hybrid Electric Vehicles on a Residential Distribution Grid," *IEEE Trans. Power Syst.*, vol. 25, no. 1, pp. 371–380, Feb. 2010.

[5] S. Deilami *et al.*, "Real-Time Coordination of Plug-In Electric Vehicle Charging in Smart Grids to Minimize Power Losses and Improve Voltage Profile," *IEEE Trans. Smart Grid*, vol. 2, no. 3, pp. 456–467, Sep. 2011.

[6] E. Sortomme, M. M. Hindi, S. D. J. MacPherson, and S. S. Venkata, "Coordinated Charging of Plug-In Hybrid Electric Vehicles to Minimize Distribution System Losses," *IEEE Trans. Smart Grid*, vol. 2, no. 1, pp. 198–205, Mar. 2011.

[7] Y. Cao *et al.*, "An Optimized EV Charging Model Considering TOU Price and SOC Curve," *IEEE Trans. Smart Grid*, vol. 3, no. 1, pp. 388–393, Mar. 2011.

[8] W. Su and M. Y. Chow, "Performance Evaluation of an EDA-Based Large-Scale Plug-In Hybrid Electric Vehicle Charging Algorithm," *IEEE Trans. Smart Grid*, vol. 3, no. 1, pp. 308–315, Mar. 2012.

[9] D. P. Tuttle and R. Baldick, "The Evolution of Plug-In Electric Vehicle-Grid Interactions," *IEEE Trans. Smart Grid*, vol. 3, no. 1, pp. 500–505, Mar. 2012.

[10] K. Clement-Nyns, E. Haesen, and J. Driesen, "The Impact of Vehicle-to-grid on the Distribution Grid," *Electr. Power Syst. Res.*, vol. 81, no. 1, pp. 185–192, Jan. 2011.

[11] A. Y. Saber and G. K. Venayagamoorthy, "Plug-in Vehicles and Renewable Energy Sources for Cost and Emission Reductions," *IEEE Trans. Ind. Electron.*, vol. 58, no. 4, pp. 1229–1238, Apr. 2011.

[12] IEEE 2030, "Guide for Smart Grid Interoperability of Energy Technology and Information Technology Operation with the Electric Power System (EPS), and End-Use Applications and Loads," *IEEE Standards Association*, Sep. 2011.

[13] P. Palensky and D. Dietrich, "Demand Side Management: Demand Response, Intelligent Energy Systems, and Smart Loads," *IEEE Trans. Ind. Inf.*, vol. 7, no. 3, pp. 381–388, Aug. 2011.

[14] M. Lévesque, D. Xu, G. Joós, and M. Maier, "Co-Simulation of PEV Coordination Schemes over a FiWi Smart Grid Communications Infrastructure," in *Proc., IEEE Ind. Electron. Soc. Annu. Conf. (IECON)*, Montreal, QC, Canada, Oct. 2012.

[15] M. Lévesque, D. Xu, M. Maier, and G. Joós, "Communications and Power Distribution Network Co-Simulation for Multidisciplinary Smart Grid Experimentations," in *Proc., SCS/ACM Spring Simulation Multi-Conf.*, Orlando, FL, USA, Mar. 2012.

[16] M. Maier, M. Lévesque, and L. Ivănescu, "NG-PONs 1&2 and Beyond: The Dawn of the Über-FiWi Network," *IEEE Netw.*, vol. 26, no. 2, pp. 15–21, March/April 2012.

[17] S. Shao, M. Pipattanasomporn, and S. Rahman, "Grid Integration of Electric Vehicles and Demand Response With Customer Choice," *IEEE Trans. Smart Grid*, vol. 3, no. 1, pp. 543–550, Mar. 2012.

[18] American National Standards Institute, "National Electrical Manufacturers Association (NEMA) ANSI C84.1-1995-American National Standard for Electric Power Systems and Equipment-Voltage Ratings (60 Hertz)," *American Nat. Standards Inst., Nat. Elect. Manufacturers Assoc.*, 2006.

[19] D. Wu, D. C. Aliprantis, and L. Ying, "Load Scheduling and Dispatch for Aggregators of Plug-in Electric Vehicles," *IEEE Trans. Smart Grid*, vol. 3, no. 1, pp. 368–376, Mar. 2012.

[20] R. J. Bessa, M. A. Matos, F. J. Soares, and J. A. P. Lopes, "Optimized Bidding of a EV Aggregation Agent in the Electricity Market," *IEEE Trans. Smart Grid*, vol. 3, no. 1, pp. 443–452, Mar. 2012.

[21] E. Sortomme and M. A. El-Sharkawi, "Optimal Scheduling of Vehicle-to-Grid Energy and Ancillary Services," *IEEE Trans. Smart Grid*, vol. 3, no. 1, pp. 351–359, Mar. 2012.

[22] S. Han, S. Han, and K. Sezaki, "Development of an Optimal Vehicle-to-Grid Aggregator for Frequency Regulation," *IEEE Trans. Smart Grid*, vol. 1, no. 1, pp. 65–72, 2010.

[23] J. Xu and V. W. S. Wong, "An Approximate Dynamic Programming Approach for Coordinated Charging Control At Vehicle-to-Grid Aggregator," in *Proc., IEEE International Conf. on Smart Grid Communications*, Brussels, Belgium, Oct. 2011, pp. 279–284.

[24] W. H. Kersting, "Radial Distribution Test Feeders," *IEEE Trans. Power Syst.*, vol. 6, no. 3, pp. 975–985, Aug. 1991.

[25] M. Duvall, "Advanced Batteries for Electric-Drive Vehicles," *Final Rep. 1009299, Elect. Power Res. Inst.*, May 2004.

[26] W. X. Shen, C. C. Chan, E. W. C. Lo, and K. T. Chau, "Estimation of Battery Available Capacity under Variable Discharge Currents," *J. Power Sources*, vol. 103, no. 2, pp. 180–187, Mar. 2002.

[27] SAE J1772, "Electric Vehicle Conductive Charge Coupler," *SAE Recommended Practice*, 2009.

[28] M. Lévesque, M. Maier, Y. Desai, and G. Joos, "Adaptive Admission Control for a Smart Grid FiWi Communications Network facing Power Blackouts during a DDoS Attack," in *Proc., IEEE Green Technologies Conference*, Tulsa, OK, USA, Apr. 2012.